

# Mortality Inferences from Estimated Life-Table Aging Rates in a Gamma-Gompertz-Makeham framework

Filipe Ribeiro\*<sup>1,2</sup> and Trifon I. Missov<sup>2,3</sup>

<sup>1</sup>CIDEHUS.UE, University of Évora, Palácio do Vimioso, 7002-554, Évora, Portugal

<sup>2</sup>Max Planck Institute for Demographic Research, Konrad-Zuse-Str. 1, D-18057 Rostock, Germany

<sup>3</sup>Institute of Sociology and Demography, University of Rostock, Ulmenstr. 69, D-18057 Rostock, Germany

\* E-mail: fribeiro@uevora.pt

March 24, 2014

## Abstract

*We calculate life-table aging rates for overall and cause-specific mortality by estimating a gamma-Gompertz-Makeham (ΓGM) model and taking advantage of LAR's parametric representation by Vaupel and Zhang (2010). For different HMD countries we study how the evolution of estimated LAR patterns (for overall mortality or specific causes of death) could explain observed 1) life expectancy dynamics, and 2) mortality improvement or deterioration at different ages. We compare our findings across countries (data from HMD) and major causes of death (data from WHO).*

## 1. Introduction

Horiuchi and Coale (1990) proposed a mortality measure, named later (Horiuchi & Wilmoth, 1997; Carey & Liedo, 1998) the life-table aging rate (LAR), which captures the age-specific rate of mortality change for a given population. The individual rate of aging, defined as the relative derivative of the baseline hazard of death from senescent causes, is a different characteristic, which is constant if the aging process is captured by a Gompertz curve.

Gampe (2010) acknowledges a levelling-off of human mortality at ages 110-114. If a mortality plateau exists, then it speaks in favor of a model with a Gompertz-Makeham baseline  $\mu_x = ae^{bx} + c$  (Gompertz 1825; Makeham 1860), where  $a$  measures the mortality level at the starting adult age,  $b$  is the individual rate of aging itself, and  $c$  captures the risk of dying that is not associated with the aging process. If, in addition, the model incorporates unobserved heterogeneity (frailty), captured by a gamma distribution with a unit mean and  $\gamma$  variance, we get the gamma-Gompertz-Makeham frailty model (Vaupel et al. 1979), which we will shortly address as the  $\Gamma$ GM. If we estimate its parameters, *i.e.*,  $a$ ,  $b$ ,  $c$  and  $\gamma$ , we can take advantage of the LAR representation by Vaupel and Zhang (2010) to estimate the population rate of aging (LAR).

Previous research (Horiuchi, Cheung and Robine, 2012) focused on reconstructing model-based LARs by fitting a Kannisto model for homogeneous populations. In this paper we focus on a  $\Gamma$ GM heterogeneous model to reflect the perception that populations consist of individuals that share the same baseline hazard, to which they are susceptible in a different (random) way.

In this article we first fit the  $\Gamma$ GM model to four countries: two from Southern Europe (Spain and Portugal), one from Western Europe (France), and one from Northern Europe (Sweden). We based our choice on the qualitatively different patterns of life-expectancy evolution over time. France and Sweden register high life expectancy at birth in the 1950s, but its rate of increase drops in the following decades. Spain and Portugal, on the other hand, experience a lower life expectancy at birth in the 1950s, but the rates of increase surpass the ones for the life expectancy leaders at the time. As a result the two countries caught up (the values of life expectancy in Spain even surpassed the ones registered in Sweden).

Second, we elaborate on the relationship between the estimated LARs and the rate of life expectancy increase in the chosen countries, as well as show how the estimated LARs reflect the age patterns of mortality deceleration – not only for the overall mortality, but also across causes of death (COD). At the same time we illustrate how well the LAR formula by Vaupel and Zhang (2010), which uses the estimated  $\Gamma$ GM parameters, fits the actual LAR.

Third, we test the heterogeneity hypothesis by Horiuchi and Wilmoth (1998) that a) deceleration occurs for the most major CODs, being less pronounced for CODs with lower death rates; and b) mortality deceleration should occur at later ages due to selection effects.

## 2. Method

The life-table aging rate, defined as (Horiuchi and Coale 1990)

$$\bar{b}(x) = \frac{1}{\mu_x} \frac{d\mu_x}{dx} = \frac{d \ln \mu_x}{dx}, \quad (1)$$

measures the rate of aging at age  $x$  for a population, whose mortality follows a hazard function  $\mu_x$ . In this study we take advantage of the  $\Gamma$ GM model developed by Vaupel *et al.* (1979) and apply it to single years for Spain, Portugal, France, and Sweden. The  $\Gamma$ GM population hazard at age  $x$  is captured by:

$$\mu_x = \frac{a e^{bx}}{1 + \frac{\gamma a}{b}(e^{bx} - 1)} + c. \quad (2)$$

where,  $a$  is the starting level of mortality,  $b$  the individual rate of aging, and  $c$  the Makeham term. The inclusion of Makeham's  $c$ , allows the distinction between extrinsic mortality from the one caused by the aging process, which is captured by the Gompertz part  $ae^{bx}$ . The inclusion of  $c$  is important for capturing the bell-shaped pattern of  $\bar{b}(x)$  as “not all monotonically increasing logistic  $\mu_x$  result in bell-shaped  $\bar{b}(x)$  patterns” and “if the factor  $c$  is excluded from the individual-level equation, then the resulting aggregate-level  $\mu_x$  function does not lead  $\bar{b}(x)$  to a bell-shaped pattern” (Horiuchi & Coale, 1990).

If we estimate the  $\Gamma$ GM parameters  $a$ ,  $b$ ,  $c$  and  $\gamma$ , we can take advantage of the LAR representation by Vaupel and Zhang (2010):

$$\bar{b}(x) = b \left(1 - \frac{c}{\mu_x}\right) - \gamma \left(1 - \frac{c}{\mu_x}\right) (\mu_x - c). \quad (3)$$

The age at which the relative derivative of  $\mu_x$  reaches its maximum is the age when mortality starts to decelerate. In a  $\Gamma$ GM framework the age of mortality deceleration is given by

$$x^* = \frac{1}{b} \ln \left( \frac{(b + c \gamma) c}{2 a b} + \frac{\sqrt{(b + c \gamma) c \gamma ((b + c \gamma) c - 4 b (a \gamma - b))}}{2 a b \gamma} \right). \quad (4)$$

The fitting procedure is based on the standard assumption for aggregate mortality data  $D(x) \sim \text{Poisson}(E(x) * \mu_x)$  (Brillinger, 1986), where  $D(x)$  denotes the death counts and  $E(x)$  the exposures at age  $x$ . For each year (independently) we maximize a Poisson log-likelihood:

$$\ln L(a, b, \gamma, c) = \sum_x [D(x) * \ln \mu_x - E(x) * \mu_x] \quad (5)$$

We focus on the last 100 years of mortality history, but always taking into account the limitations (availability and time range) associated with (especially COD) data. For each selected country, for each year in the available period, for overall mortality and COD data we estimate the LAR by fitting a  $\Gamma$ GM model beyond age 65.

To elaborate on the relationship between estimated LARs and life expectancy dynamics, we differentiate between different period segments on the overall timeline, i.e., we estimate independently different regression lines that incorporate a piece-wise linear relationship between life expectancy and calendar year. This results in two (or more) line segments. Assuming a changing point  $i$ , the relationship between the different life expectancies ( $e_i$ ) registered across years and the calendar year itself ( $y_i$ ) is captured by:

$$e_i = \alpha + \beta_1 y_i + \beta_2 (y_i - \psi)_+ \quad (6)$$

Where  $\alpha$  is the intercept,  $\beta_1$  is the first segment slope,  $\beta_2$  the difference-in-slopes for the second segment,  $\psi$  denotes the breakpoint, and  $(y_i - \psi)_+ = (y_i - \psi) * I(y_i > \psi)$  (Muggeo, 2003). The indicator function  $I(\cdot)$  equals one when the condition in its argument is true. When the model does not detect a breakpoint, we end up with a simple linear regression model, i.e.,  $\psi$  does not exist and  $\beta_2$  is a statistical zero.

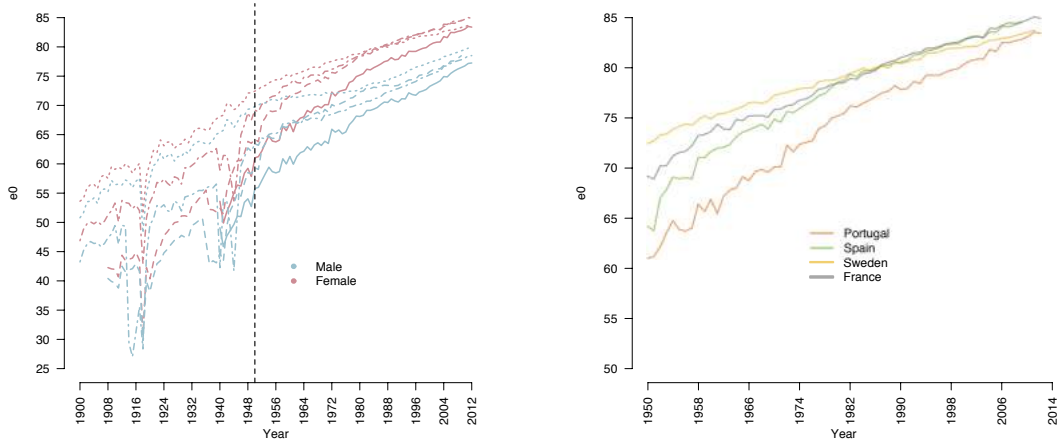
### 3. Data

We use data for the overall mortality from the *Human Mortality Database* (HMD: [www.mortality.org](http://www.mortality.org)) and cause-of-death data from the *World Health Organization Mortality Database* (WHOMD). As explained in the introductory section, country selection was based on the qualitatively different patterns of life-expectancy evolution over time, where France and Sweden, registering a high life expectancy at birth already in the 1950s, experienced a drop in the life expectancy rate of increase in the following decades; Spain and Portugal experienced a low life expectancy at birth in the 1950s, but the rates of increase surpassed the life expectancy leaders at the time, and the two countries caught up and the values of life expectancy in Spain even surpassed the ones registered in Sweden (*Figure 1*).

WHOMD cause-of-death (COD) data are only available by five-year age groups and once that we extract death counts according to ICD10, our timeline in what concerns to COD is restricted essentially to the last available decade (depending on the country). We leave Portugal out of the analysis by COD as the last open-end age group is 85+ and not 95+. To avoid any lack of representativeness, we work with major COD groups: 1) Neoplasms, 2) Ischaemic Heart Diseases; 3) Cerebrovascular Diseases; 4) Remaining Diseases of the Circulatory System; 5) Diseases of the Respiratory System; 6)

Diseases of the Digestive System; 7) External Causes of Death; and 8) Remaining Causes of Death. Following the WHO recommendation (1977), we base our research on the *underlying cause of death*, i.e., the disease or injury, which initiated the series of events that lead to death.

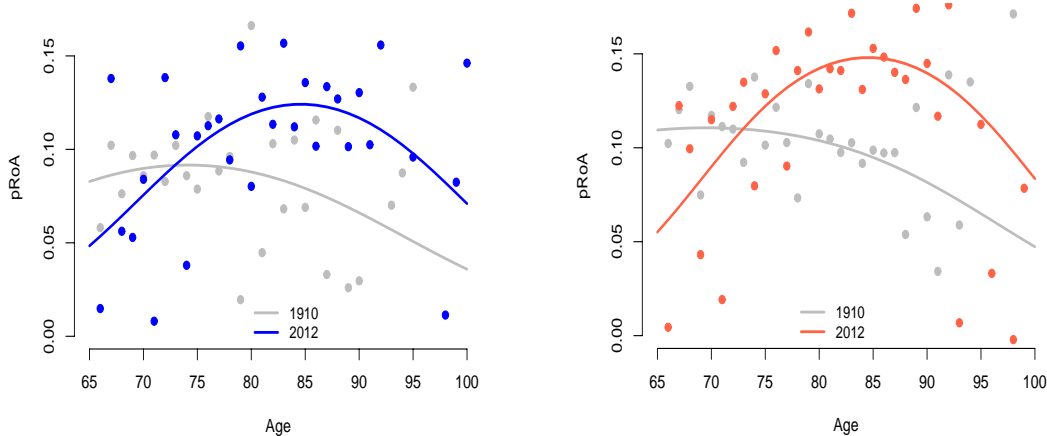
**Figure 1:** The evolution of Life Expectancy at Birth in the selected countries  
 Panel 1: Pattern by sex  
 Panel 2: The female example



#### 4. Results

By fitting a  $\Gamma$ GM model from age 65 onwards, we estimate individual ( $b$ ) and population rates of aging ( $\bar{b}$ , i.e. LAR) by country, gender, and cause of death. Results for France and Spain, presented in *Figure 2* indicate that the  $\Gamma$ GM model-based LAR  $\bar{b}$  fits well observed LAR (calculated from life-table mortality rates). At the same time, it captures the observed shift in the age of mortality deceleration between 1910 and 2012 in the French case, and from 1960 to 2009 in the Spanish one, for both sexes, and it seems to confirm point b) of the heterogeneity hypothesis: with increasing lifespans, mortality deceleration shifts and occurs always at older ages.

**Figure 2:** Empirical and model-based population rate of aging (pRoA)  
 Panel 1: Male, France  
 Panel 2: Female, France



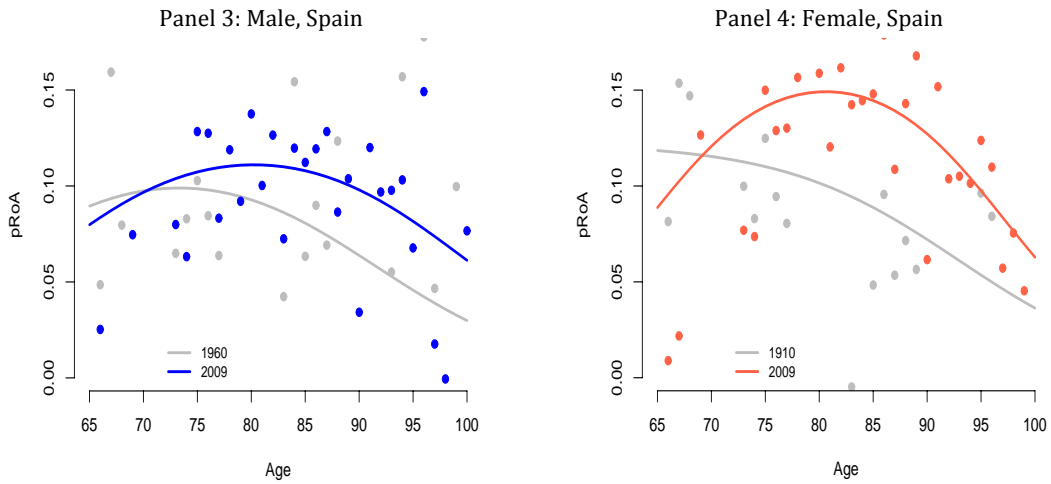
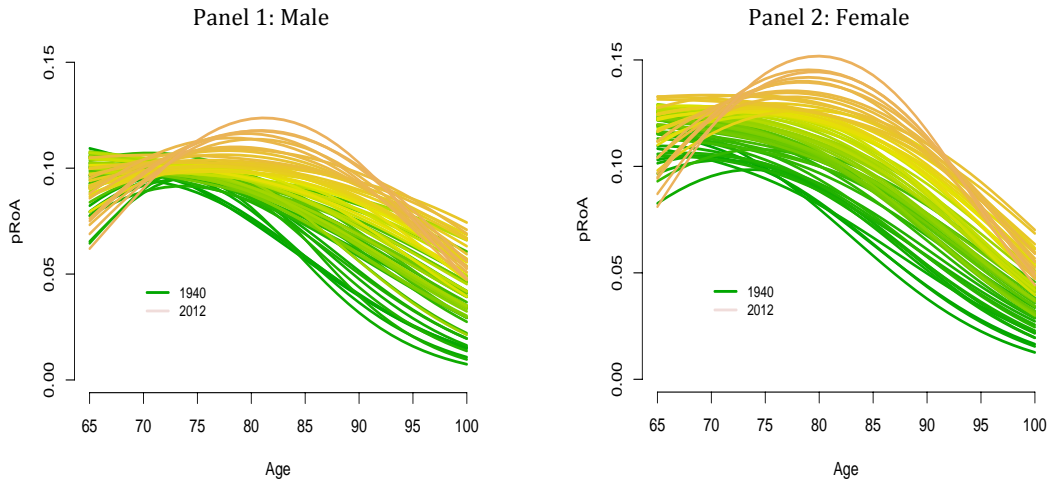


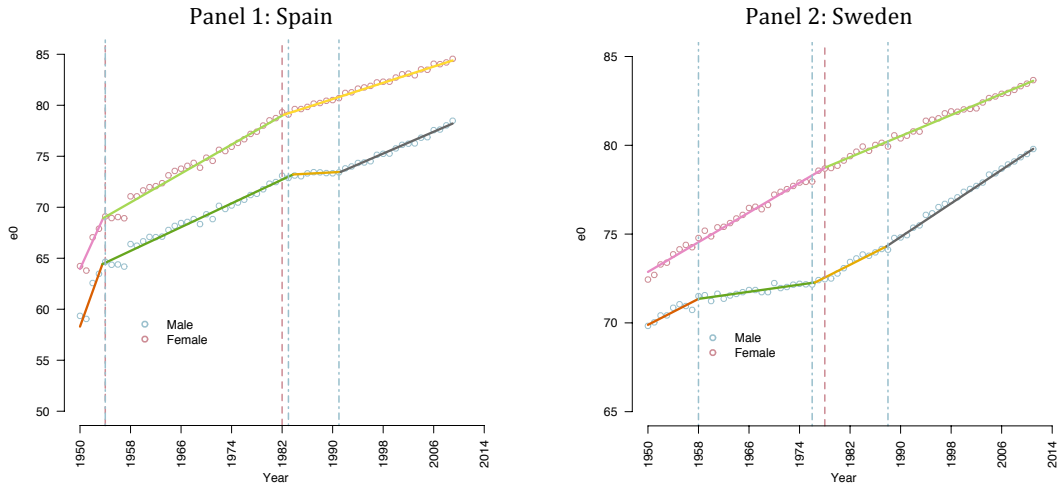
Figure 3 also supports point b) of the heterogeneity hypothesis. Model-based LAR for Portugal detects a shift of the age of mortality deceleration to older ages with time, and that is transversal to both sexes. It seems that mortality deceleration starts later for females than for males. This might be related to the life expectancy gap between sexes.

**Figure 3:** Model-based population rate of aging (pRoA) for Portugal



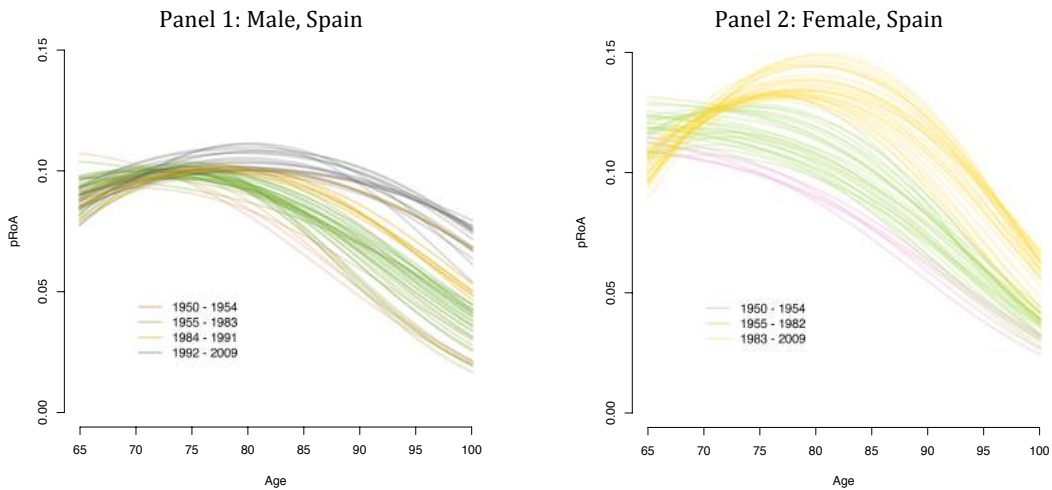
To elaborate on the connection between the evolution of life expectancy at birth and the changes across time on the age of mortality deceleration, we study the outcomes of estimating (6). Figure 4 presents the estimated breakpoints for Spain (panel 1) and Sweden (panel 2): males and females. In both countries are the females that register fewer “partitions” of the slope, and men are catching up, i.e., have a steeper slope of life expectancy increase (only in the last segment).

**Figure 4: Segmented evolution of Life Expectancy at Birth**



Results presented in *Figure 5* correspond to the model-based LAR presented by the different significant estimated segments. With those obtained results for LAR (pRoA), we can clearly observe a shift to the right in the age of mortality deceleration ( $x^*$ ), reinforcing what was said about the heterogeneity hypothesis and simultaneously, identify different patterns for the pRoA according with the different paces of increase in life expectancy at birth estimated by the segmented regression model (equation 6).

**Figure 5: Model-based population rate of aging (pRoA)**



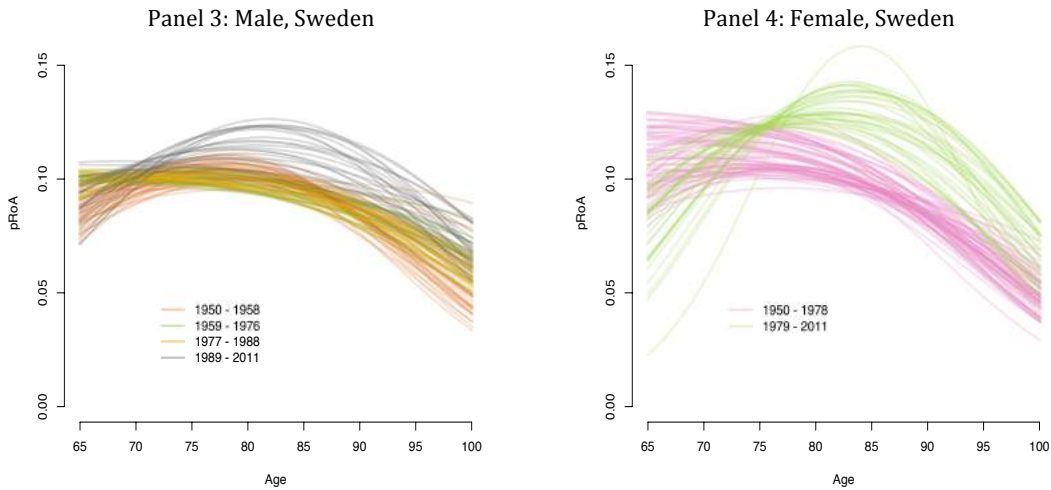
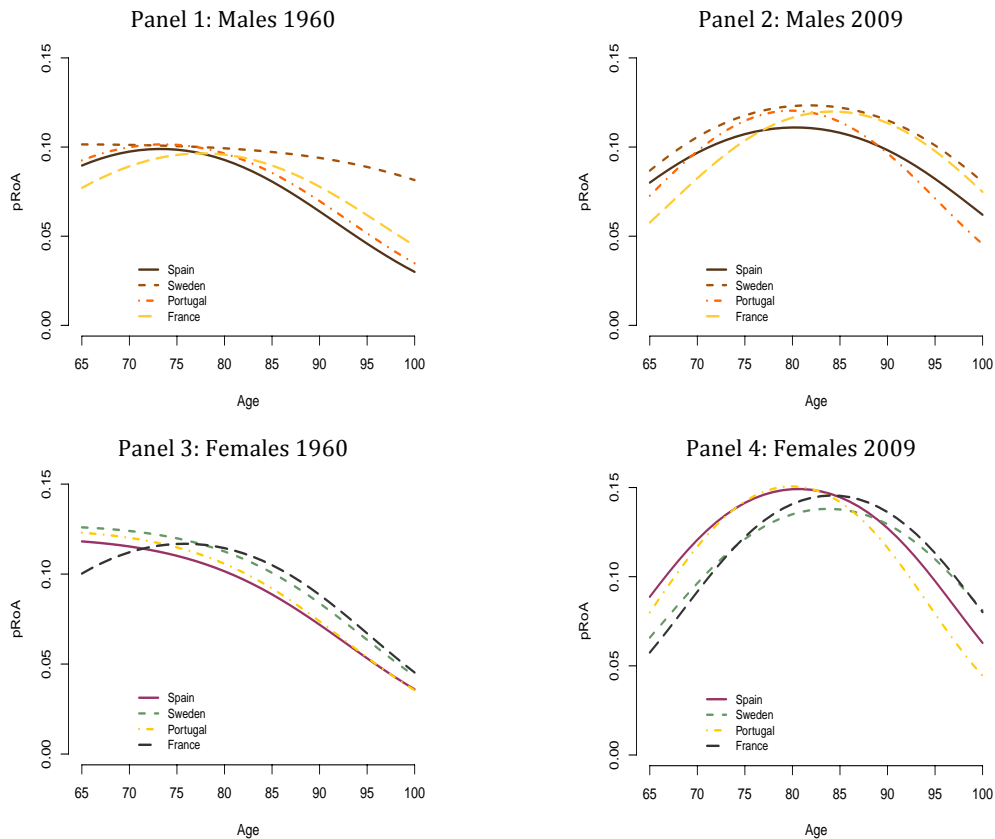


Figure 6, presents the obtained results for the four studied countries, and, at a first glance, it seems that the shift registered in mortality deceleration for France is transversal to all the other three countries, independently of the sex. However, these results also show that despite the presentation of a similar pattern in the evolution of LAR across countries and sexes, the age of mortality decrease appear to be different in each of them. This suggests that life expectancy can be related to the evolution of the age of mortality deceleration, and at this point, we can now affirm that the pace of increase in life expectancy is effectively captured by the age of mortality deceleration.

**Figure 6:** Model-based population rate of aging (pRoA) by sex and country





As already pointed out, fitting  $\Gamma$ GM to COD data is sometimes problematic since for some causes of death in some age intervals the sample size is small. That is why we will illustrate our findings on the example of France, whose large population size facilitates precise statistical estimation of parameters. *Figure 7* presents both the empirical (observed) LAR and the  $\Gamma$ GM one for Neoplasms in 2009. Like the ones for overall mortality, the model-based COD-specific LARs approximate the life-table LARs very well. *Figure 7* also shows that in 2009 the age of mortality deceleration is higher for females than for males.

**Figure 7:** Empirical and model-based LAR for Neoplasms, France 2009

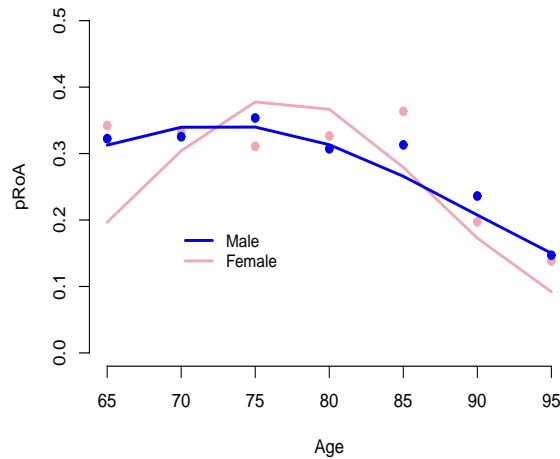
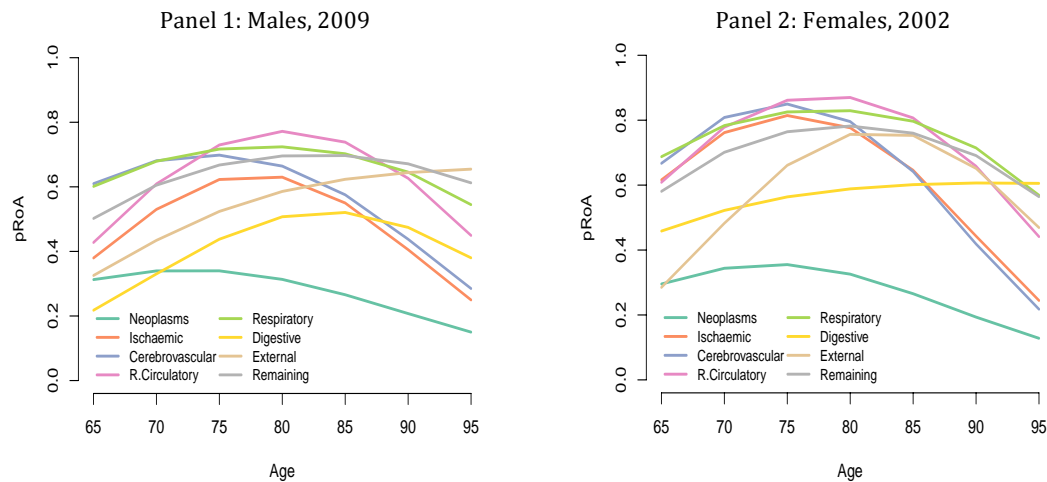


*Figure 8* presents the  $\Gamma$ GM LARs for French males and females by COD in 2002 (panel 2) and 2009 (panel1). Despite the observed differences in the age of mortality deceleration among different CODs and between genders, we can clearly identify the flatter LAR-pattern for Neoplasms (both sexes) and Digestive Diseases (females) and, in general, their LARs' lower values in comparison to the other CODs. As Horiuchi and Coale (1990) suggest, this should be related to lower corresponding death rates. As a result, we know that deaths caused by neoplasms occur essentially before age 65 and deaths caused by digestive system diseases are more common in males than females, hence, confirming point a) of the heterogeneity hypothesis.

**Figure 8:** Model-based LAR for France



## 5. Conclusion

$\Gamma$ GM model-based LARs (for overall mortality and by COD) seem to be consistent with the heterogeneity hypotheses advanced by Horiuchi and Coale (1990) as the age of mortality deceleration shifts to older ages with time. The  $\Gamma$ GM model-based LAR (Vaupel and Zhang 2010) fits observed LAR with high accuracy and captures the connection relationship between the observed shift and the rate of life expectancy increase in the four chosen countries. Presented results for overall mortality are statistically more accurate because the analysis is based on a large number of observations in each age group. Although COD data are organized by five-year age groups, we sometimes run into problems associated with low sample sizes, which might influence the accuracy of  $\Gamma$ GM parameter estimates. Disaggregation of population data by causes of death, can aid further understanding the strength of the relationship between LAR patterns and life-expectancy dynamics across countries and by gender.

## References

- Brillinger, D.R. (1986). The natural variability of vital rates and associated statistics. *Biometrics* 42, 693-734.
- Carey, J.R. & Liedo, P. (1998). Sex-specific life table aging rates in large medfly cohorts. *Experimental Gerontology* 30, 315-325.
- Gampe, J. (2010). Human mortality beyond age 110. In: H. Maier, J.G.B. Jeune, J.M. Robine, and J.W. Vaupel (eds), *Supercentenarians*, Heidelberg, Springer, 219-230.
- Gompertz, B. (1825). On the nature of the function expressive of the law of human mortality, and on a new mode of determining the value of life contingencies. *Philosophical Transactions of the Royal Society of London* 115, 513-585.
- Horiuchi, S., Cheung, S.L.K., Robine, J.M. (2012). Cause-of-death decomposition of old-age mortality compression. In: 2012 annual meeting of the Population Association of America (PAA).
- Horiuchi, S. & Wilmoth, J.R. (1997). Age patterns of life table aging rate for major causes-of-death in Japan, 1951-1990. *Journal of Gerontology, Biological Sciences*, 52A(1), B67--B77.
- Horiuchi, S. & Coale, A.J. (1990). Age patterns of mortality for older women: An analysis using the age-specific rate of mortality change with age. *Mathematical Population Studies*, 2(4), 245--267.
- Makeham, W. M. (1860). On the law of mortality. *Journal of the institute of actuaries* 13, 283--287.
- Muggeo, V. (2003). Estimating regression models with unknown break-points. *Statistics in Medicine* 22, 3055-3071.
- Vaupel, J.W. (2010). Biodemography of human aging. *Nature* 7288, 536-542.
- Vaupel, J.W. & Zhang, Z. (2010). Attrition in heterogeneous cohorts. *Demographic Research*, Volume 23, Article 26, 737-748.
- Vaupel, J.W., Manton, K., Stallard, E. (1979). The impact of heterogeneity in individual frailty on the dynamics of mortality. *Demography* 16, 855-860.
- World Health Organization (1977). Manual of the International Statistical Classification of Diseases, Injuries, and Causes of Death, based on recommendations of the Ninth Revision Conference, 1975 Geneva: World Health Organization (WHO).